HHS Public Access

Author manuscript

Nature. Author manuscript; available in PMC 2009 July 17.

Published in final edited form as:

Nature. 2008 July 24; 454(7203): 538–542. doi:10.1038/nature07065.

Oligomerization of STIM1 couples ER calcium depletion to CRAC channel activation

Riina M. Luik[*], **Bin Wang**[1,*], **Murali Prakriya**[2,*], **Minnie M. Wu**, and **Richard S. Lewis**[3]

Department of Molecular and Cellular Physiology, Stanford University School of Medicine, Stanford, CA 94305

Ca^{2+} release-activated Ca^{2+} (CRAC) channels generate sustained Ca^{2+} signals that are essential for a range of cell functions, including antigen-stimulated T lymphocyte activation and proliferation1, 2. Recent studies3 have revealed that the depletion of Ca^{2+} from the endoplasmic reticulum (ER) triggers the oligomerization of STIM1, the ER Ca^{2+} sensor, and its redistribution to ER-plasma membrane (ER-PM) junctions4–8 where the CRAC channel subunit Orai1 accumulates in the plasma membrane and CRAC channels open9–12. However, how the loss of ER Ca^{2+} sets into motion these coordinated molecular rearrangements remains unclear. Here we define the relationships among $[Ca^{2+}]_{ER}$, STIM1 redistribution, and CRAC channel activation and identify STIM1 oligomerization as the critical $[Ca^{2+}]_{ER}$–dependent event that drives store-operated Ca^{2+} entry (SOCE). In cells expressing an ER-targeted Ca^{2+} indicator, CRAC channel activation and STIM1 redistribution follow the same function of $[Ca^{2+}]_{ER}$, with a $K_{1/2}$ of ~200 μM and a Hill coefficient of ~4. Because STIM1 binds only a single Ca^{2+} ion5, the high apparent cooperativity suggests that STIM1 must first oligomerize to enable its accumulation at ER-PM junctions. To assess directly the causal role of STIM1 oligomerization in SOCE, we replaced the luminal Ca^{2+}-sensing domain of STIM1 with the rapamycin-binding proteins FRB or FKBP. A rapamycin analog oligomerizes the fusion proteins and causes them to accumulate at ER-PM junctions and activate CRAC channels without depleting Ca^{2+} from the ER. Thus, STIM1 oligomerization is the critical transduction event through which Ca^{2+} store depletion controls store-operated Ca^{2+} entry, acting as a switch that triggers the self-organization and activation of STIM1-Orai1 clusters at ER-PM junctions.

The defining feature of store-operated channels is their activation in response to ER Ca^{2+} ($[Ca^{2+}]_{ER}$) depletion. However, their sensitivity to $[Ca^{2+}]_{ER}$ and the factors that determine this sensitivity have never been established, largely because of the technical difficulty of quantifying $[Ca^{2+}]_{ER}$. To address this issue we generated a Jurkat T cell line stably expressing the Ca^{2+}-sensitive cameleon protein, YC4.2er. YC4.2er is selectively retained in the ER, as shown by its colocalization with the resident ER protein calnexin but not with mitochondrial or Golgi markers, and by its functional response to agents that deplete ER

[3]To whom correspondence and proofs should be addressed: Richard S. Lewis, Beckman Center B-121A, Stanford University School of Medicine, Stanford, CA 94305, tel 650-723-9615, fax 650-498-5286, em: rslewis@stanford.edu.

[*]These authors contributed equally

[1]Present address: Department of Physiology, University of Texas Health Science Center at San Antonio, San Antonio, TX 78229.

[2]Present address: Department of Molecular Pharmacology and Biological Chemistry, Feinberg School of Medicine, Northwestern University, Chicago, IL 60611

Ca^{2+} (Fig. 1a and Supp. Fig. 1). *In situ* calibration of the YC4.2er FRET signal indicates a responsivity to $[Ca^{2+}]_{ER}$ in the range of ~1 μM to >1 mM (Supp. Fig. 2).

To determine the dependence of CRAC channel activation on $[Ca^{2+}]_{ER}$, we measured I_{CRAC} in perforated-patch recordings from Jurkat YC4.2er cells treated with cyclopiazonic acid (CPA), a reversible SERCA inhibitor. CPA evokes a time-dependent decline in $[Ca^{2+}]_{ER}$ in parallel with the activation of I_{CRAC} measured in the same cell (Fig. 1a). However, because I_{CRAC} responds slowly to rapid changes of $[Ca^{2+}]_{ER}$, non-stationary measurements like these will distort estimates of the true $[Ca^{2+}]_{ER}$ dependence of the CRAC channel. For this reason we determined instead the $[Ca^{2+}]_{ER}$-I_{CRAC} relationship under steady-state conditions, by pretreating cells with 0.5–20 μM CPA for 8–15 min in the absence of extracellular Ca^{2+} to generate a range of constant $[Ca^{2+}]_{ER}$ values. This passive depletion approach also minimizes spatial variations of $[Ca^{2+}]_{ER}$, allowing the $[Ca^{2+}]_{ER}$ dependence of SOCE to be determined from whole-cell YC4.2er measurements. Following readdition of 20 mM Ca^{2+} to the bath, current was monitored during brief hyperpolarizations from the resting potential of +30–50 mV at constant $[Ca^{2+}]_{ER}$ (Fig. 1b). The current was identified as I_{CRAC} based on its delayed response to extracellular Ca^{2+} reflecting Ca^{2+}-dependent potentiation (Fig. 1b), an inwardly rectifying I/V relation (Fig. 1b), and extremely low current noise17. Measurements from 40 cells show that I_{CRAC} is a steep function of $[Ca^{2+}]_{ER}$ with a $K_{1/2}$ of 169 μM and a Hill coefficient (n_H) of 4.2 (Fig. 1c). Interestingly, a decline of >100 μM from the resting $[Ca^{2+}]_{ER}$ of ~400 μM is required to initiate CRAC channel opening in these cells, which may help explain the ability of IP_3 to release small amounts of ER Ca^{2+} without activating I_{CRAC} in some cells18.

We next addressed the source of the CRAC channel's steep dependence on $[Ca^{2+}]_{ER}$. Because STIM1 is known to be the Ca^{2+} sensor for SOCE6, 7 and its redistribution to ER-PM junctions is linked to I_{CRAC} activation6, 8, 11, we measured the dependence of STIM1 redistribution on $[Ca^{2+}]_{ER}$. Exposure to 0.5–3 μM CPA for > 8 min causes a partial redistribution of Cherry-STIM1 to the cell periphery, which can be seen by widefield imaging at the cell equator (Fig. 2a). We quantified the redistribution of Cherry-STIM1 as the ratio of the mean peripheral fluorescence to the mean total fluorescence (Fig. 2b); this method gives results that agree quantitatively with TIRF measurements of STIM1 puncta (Supp. Fig. 3) while facilitating the separation of the cameleon and Cherry fluorescence signals (see Supplementary Information). Measurements from 41 cells show that STIM1 redistribution is a steep function of $[Ca^{2+}]_{ER}$ that closely resembles that of I_{CRAC} activation, with a $K_{1/2}$ of 187 μM and a Hill coefficient of 3.8 (Fig. 2c). The value of $K_{1/2}$ is close to the binding affinity of the recombinant EF-hand/SAM domain of STIM1 measured *in vitro* (K_D = 200–600 μM; ref 5), consistent with its role as an ER Ca^{2+} sensor. Importantly, the close correspondence between the STIM1 and I_{CRAC} curves indicates that CRAC channels open in direct proportion to the concentration of STIM1 at ER-PM junctions and that the CRAC channel derives its highly nonlinear dependence on $[Ca^{2+}]_{ER}$ from the ER Ca^{2+} dependence of STIM1 redistribution. A recent study of HeLa cells found a similar dependence of STIM1 redistribution on $[Ca^{2+}]_{ER}$ (ref 13). In that study, the homolog STIM2 redistributed to ER-PM junctions at higher $[Ca^{2+}]_{ER}$ ($K_{1/2}$ = 406 μM) than did STIM1 ($K_{1/2}$ = 210 μM), and it was proposed that STIM2 functions as a homeostatic ER Ca^{2+} sensor by

activating Orai1. Our findings that I_{CRAC} and STIM1 redistribution follow the same function of $[Ca^{2+}]_{ER}$ implies that in Jurkat cells STIM2 activates at most a minor fraction of endogenous CRAC channels, consistent with its low level of expression in T cells14.

The shape of the STIM1 redistribution curve has important implications for the mechanism underlying SOCE. The Hill coefficient of ~4 shows that puncta formation is a nonlinear process with respect to $[Ca^{2+}]_{ER}$ without necessarily indicating a cooperative mechanism or that the active form of STIM1 is a tetramer. However, the high Hill coefficient implies that STIM1 puncta at ER-PM junctions do not form by the independent accretion of STIM1 monomers, which contain only a single luminal Ca^{2+} binding site5, but suggests instead that only oligomers of STIM1 can accumulate at these sites. There are two ways in which STIM1 is known to oligomerize. In resting cells STIM1 self-associates with an undetermined stoichiometry via its cytosolic coiled-coil domains15, 16; in addition, removal of Ca^{2+} from the EF-hand of STIM1 drives further oligomerization *in vitro*5 and *in vivo*4. Store-dependent oligomerization of STIM1 occurs within seconds, slightly in advance of puncta formation, and a causal role in SOCE has been hypothesized but never tested4, 5.

To address the possible role of STIM1 oligomerization in SOCE, we adopted an approach based on rapamycin-induced protein heterodimerization17, 18. We replaced the EF-SAM domain of Cherry-STIM1 with a tandem dimer of FK506-binding protein (FKBP12) or a variant of the rapamycin-binding domain of mTOR (FRB) to generate STIM1 chimeras that will heterodimerize when bound to a rapamycin analog (AP21967, or rapalog). Given that STIM1 is known to self-associate at rest15, 16, rapalog would thus be expected to link multimers containing FRB with those containing FKBP to form extended oligomers of STIM1 (Fig. 3a). We assayed oligomer formation in HEK293 cells expressing Cherry-FRB-STIM1 and Cherry-FKBP-STIM1 (abbreviated hereafter as F-STIM1) using blue native polyacrylamide gel electrophoresis (BN-PAGE)19. The >2-fold increase in apparent mass following rapalog treatment confirms its ability to oligomerize F-STIM1, and because crosslinking of monomers would be expected to at most double the mass, indicates that the resting state of FRB-STIM1 and FKBP-STIM1 is at least a dimer (Fig. 3b).

We first examined the effects of rapalog on the localization of F-STIM1 in Jurkat cells. Rapalog evoked a redistribution of F-STIM1 to the cell periphery that was complete within several minutes (Fig. 3c). Quantitative analysis shows that rapamycin triggers the redistribution of F-STIM1 as effectively as Ca^{2+} store depletion induces the redistribution of wild-type STIM1 (Fig. 3d). When examined by TIRF microscopy, the rapalog-driven peripheral accumulations of F-STIM1 (Fig. 3e) resemble the puncta of wild-type STIM1 that form in response to store depletion (Fig. 3f). Similar results were obtained in HEK293 cells. Rapalog did not affect the localization of wild-type STIM1 (Fig. 3g), nor did it deplete Ca^{2+} stores (see below). Finally, rapalog-induced F-STIM1 puncta co-localize with store depletion-induced GFP-STIM1 puncta in the same cell, confirming that rapalog causes F-STIM1 to accumulate at the same ER-PM junctions where STIM1 and Orai1 are known to interact. Thus, we conclude that oligomerization of STIM1 is sufficient to drive the redistribution of STIM1 to ER-PM junctions.

Heterodimerization of FRB-STIM1 and FKBP-STIM1 also activates endogenous CRAC channels. Rapalog elevated the mean resting $[Ca^{2+}]_i$ in Jurkat cells expressing F-STIM1 (Cherry-positive cells) from 170 ± 11 nM (untreated; n = 61) to 388 ± 45 nM (Fig. 4a; n = 45), but did not affect $[Ca^{2+}]_i$ in untransfected Jurkat cells. The elevated basal $[Ca^{2+}]_i$ was dependent on extracellular Ca^{2+} (Fig. 4a) and was inhibited by 2-APB and low concentrations of La^{3+} (Supp. Fig. 4), consistent with constitutive Ca^{2+} entry through open CRAC channels. Importantly, TG released similar amounts of ER Ca^{2+} in rapalog-pretreated and resting cells, indicating that rapalog stimulates Ca^{2+} entry without depleting Ca^{2+} stores (Fig. 4a). Whole-cell recordings with a high-$[Ca^{2+}]$ pipette solution designed to minimize store depletion confirmed that heterodimerization of FRB-STIM1 and FKBP-STIM1 directly activates I_{CRAC}. In untreated Jurkat cells expressing F-STIM1, I_{CRAC} was negligible upon breaking in to the whole-cell configuration and developed slowly to a small amplitude, presumably in response to partial store depletion. In contrast, in rapamycin-pretreated cells with visible puncta, large inward currents were evident immediately upon breaking in (Fig. 4b) and displayed essential features of I_{CRAC}, including a dependence on extracellular Ca^{2+}, inwardly rectifying current-voltage relation (Fig. 4c), low current noise, rapid Ca^{2+}-dependent inactivation, and inhibition by 2-APB and La^{3+} (Supp. Fig. 4). The mean current amplitude (2.6 ± 0.6 pA/pF, n= 9) was similar to that produced by Ca^{2+} store depletion in Jurkat cells overexpressing Cherry-STIM1 (ref 11), consistent with the comparable degrees of STIM1 and F-STIM1 redistribution in response to TG or rapalog, respectively (Fig. 3). Together, these results suggest that F-STIM1 oligomers at ER-PM junctions are fully active and provide direct evidence that the oligomerization of STIM1, independently of changes in $[Ca^{2+}]_{ER}$, is sufficient to evoke CRAC channel activation.

We have shown that STIM1 redistribution and I_{CRAC} share a steep dependence on $[Ca^{2+}]_{ER}$ and that oligomerization of F-STIM1 is sufficient to drive puncta formation and CRAC channel activation. These results define the input-output relation of the CRAC channel and identify STIM1 oligomerization as the primary transduction event through which this relation is determined. The EF hand and SAM domains of STIM1 appear to serve primarily to control the extent of oligomerization, considering that removal of Ca^{2+} causes a recombinant EF-SAM peptide to oligomerize *in vitro*5, and that the FRB and FKBP modules in F-STIM1 can effectively substitute for the EF-SAM domain and activate I_{CRAC} when crosslinked by rapalog. That the latter occurs without Ca^{2+} store depletion suggests that once STIM1 oligomerizes, all subsequent steps leading to SOCE occur independently of ER Ca^{2+}. Thus, we propose that the oligomerization of STIM1 acts as a switch to trigger the self-organization of STIM1 and Orai1 complexes at ER-PM junctions and the consequent activation of CRAC channels.

How might this oligomerization “switch” operate? In its resting state, Ca^{2+}-bound STIM1 moves freely throughout the ER membrane4 but following store depletion, STIM1 oligomers accumulate in ER subregions located 10–25 nm from the PM, close enough to allow trapping by binding to targets in the PM8. These targets have not yet been positively identified, but suggested candidates include Orai1 (refs 20, 21) or an associated protein22, and PM phospholipids4, 23. Once localized at ER-PM junctions STIM1 then promotes the accumulation of Orai1 at apposed sites, leading to channel activation11, 12, 24.

Oligomerization may promote the binding of STIM1 to its targets in two ways: an affinity-based mechanism in which a conformational change exposes a previously masked cytosolic binding domain, and an avidity-based mechanism in which clustering of the binding domains increases their local concentration at ER-PM junctions. Both of these mechanisms are likely to contribute to the assembly and function of CRAC channel complexes that constitute the final stage of the SOC activation process.

METHODS SUMMARY

$[Ca^{2+}]_{ER}$ measurements

$[Ca]_{ER}$ was measured in a Jurkat E6-1 cell line stably expressing a modified YC4er (V68L and Q69M; refs 25–27). Cells were pre-treated with CPA (0.5–20 μM) in Ca^{2+}-free Ringer's for 8–15 min, and emission intensities at 485 and 535 nm were averaged across the cell to yield a raw emission ratio. Ratios were calibrated *in situ* for every cell as described (Supplementary Information).

Heterodimerizer experiments

To generate F-STIM1, mutant FRB and tandem FKBP sequences were substituted for the EF-SAM domain (wtSTIM1 aa 35–207) in Cherry-STIM1 using plasmids provided by Ariad Pharmaceuticals (Cambridge, MA). F-STIM1 was crosslinked using 1 μM rapalog (AP21967, Ariad Pharmaceuticals). Unless indicated otherwise, cells were pre-incubated in full medium at 37°C for 30 min, with or without rapalog, and subsequent measurements were performed at 22–25°C in standard Ringer's solutions. Timelapse imaging was performed at 37°C in full medium with or without rapalog. Only cells with ~3–10% of the fluorescence of the brightest cells in each experiment were analyzed. BN-PAGE was performed essentially as described19. A mAb against the STIM1 C-terminus (1:250; Abnova, Taipei City, Taiwan) and an alkaline phosphatase-conjugated 2° antibody (1:30,000; Sigma) were used for Western blotting.

Perforated-patch and whole-cell recording

I_{CRAC} in YC4.2er cells (Fig. 1) was recorded in the perforated-patch configuration28 with 20 mM extracellular Ca^{2+}, using a stimulus of a 50-ms step to −100 mV followed by a ramp from −100 to +100 mV, delivered from a holding potential of +30 or +50 mV. Whole-cell recording of I_{CRAC} (ref 29; Fig. 4) was performed with 20 mM Ca^{2+} Ringer's, with stimuli consisting of a 100-ms step to −112 mV followed by a 100-ms voltage ramp from −112 to +88 mV applied from the holding potential of +38 mV beginning within 5 s of break-in.

Supplementary Material

Refer to Web version on PubMed Central for supplementary material.

Acknowledgments

We thank Nirav Bhakta and Diana Bautista for assistance and advice during the initial phase of these studies, Roger Tsien for the gift of cameleon YC4er, Priti Bacchawat for advice on BN-PAGE, and Ricardo Dolmetsch for comments on the manuscript. This work was supported by a grant from the National Institutes of Health (NIH) and the Mathers Charitable Foundation.

References

1. Parekh AB, Putney JW Jr. Store-operated calcium channels. Physiol Rev. 2005; 85:757–810. [PubMed: 15788710]
2. Feske S. Calcium signalling in lymphocyte activation and disease. Nat Rev Immunol. 2007; 7:690–702. [PubMed: 17703229]
3. Wu MM, Luik RM, Lewis RS. Some assembly required: constructing the elementary units of store-operated Ca^{2+} entry. Cell Calcium. 2007; 42:163–172. [PubMed: 17499354]
4. Liou J, Fivaz M, Inoue T, Meyer T. Live-cell imaging reveals sequential oligomerization and local plasma membrane targeting of stromal interaction molecule 1 after Ca^{2+} store depletion. Proc Natl Acad Sci U S A. 2007; 104:9301–9306. [PubMed: 17517596]
5. Stathopulos PB, Li GY, Plevin MJ, Ames JB, Ikura M. Stored Ca^{2+} depletion-induced oligomerization of STIM1 via the EF-SAM region: An initiation mechanism for capacitive Ca^{2+} entry. J Biol Chem. 2006; 281:35855–35862. [PubMed: 17020874]
6. Zhang SL, et al. STIM1 is a Ca^{2+} sensor that activates CRAC channels and migrates from the Ca^{2+} store to the plasma membrane. Nature. 2005; 437:902–905. [PubMed: 16208375]
7. Liou J, et al. STIM is a Ca^{2+} sensor essential for Ca^{2+}-store-depletion-triggered Ca^{2+} influx. Curr Biol. 2005; 15:1235–1241. [PubMed: 16005298]
8. Wu MM, Buchanan J, Luik RM, Lewis RS. Ca^{2+} store depletion causes STIM1 to accumulate in ER regions closely associated with the plasma membrane. J Cell Biol. 2006; 174:803–813. [PubMed: 16966422]
9. Prakriya M, et al. Orai1 is an essential pore subunit of the CRAC channel. Nature. 2006; 443:230–233. [PubMed: 16921383]
10. Vig M, et al. CRACM1 multimers form the ion-selective pore of the CRAC channel. Curr Biol. 2006; 16:2073–2079. [PubMed: 16978865]
11. Luik RM, Wu MM, Buchanan J, Lewis RS. The elementary unit of store-operated Ca^{2+} entry: local activation of CRAC channels by STIM1 at ER-plasma membrane junctions. J Cell Biol. 2006; 174:815–825. [PubMed: 16966423]
12. Xu P, et al. Aggregation of STIM1 underneath the plasma membrane induces clustering of Orai1. Biochem Biophys Res Commun. 2006; 350:969–976. [PubMed: 17045966]
13. Brandman O, Liou J, Park WS, Meyer T. STIM2 is a feedback regulator that stabilizes basal cytosolic and endoplasmic reticulum Ca^{2+} levels. Cell. 2007; 131:1327–1339. [PubMed: 18160041]
14. Oh-Hora M, et al. Dual functions for the endoplasmic reticulum calcium sensors STIM1 and STIM2 in T cell activation and tolerance. Nat Immunol. 2008; 9:432–443. [PubMed: 18327260]
15. Baba Y, et al. Coupling of STIM1 to store-operated Ca^{2+} entry through its constitutive and inducible movement in the endoplasmic reticulum. Proc Natl Acad Sci U S A. 2006; 103:16704–16709. [PubMed: 17075073]
16. Williams RT, et al. Stromal interaction molecule 1 (STIM1), a transmembrane protein with growth suppressor activity, contains an extracellular SAM domain modified by N-linked glycosylation. Biochim Biophys Acta. 2002; 1596:131–137. [PubMed: 11983428]
17. Bayle JH, et al. Rapamycin analogs with differential binding specificity permit orthogonal control of protein activity. Chem Biol. 2006; 13:99–107. [PubMed: 16426976]
18. Varnai P, Thyagarajan B, Rohacs T, Balla T. Rapidly inducible changes in phosphatidylinositol 4,5-bisphosphate levels influence multiple regulatory functions of the lipid in intact living cells. J Cell Biol. 2006; 175:377–382. [PubMed: 17088424]
19. Schägger H, von Jagow G. Blue native electrophoresis for isolation of membrane protein complexes in enzymatically active form. Anal Biochem. 1991; 199:223–231. [PubMed: 1812789]
20. Muik M, et al. Dynamic Coupling of the Putative Coiled-coil Domain of ORAI1 with STIM1 Mediates ORAI1 Channel Activation. J Biol Chem. 2008; 283:8014–8022. [PubMed: 18187424]
21. Yeromin AV, et al. Molecular identification of the CRAC channel by altered ion selectivity in a mutant of Orai. Nature. 2006; 443:226–229. [PubMed: 16921385]

22. Varnai P, Toth B, Toth DJ, Hunyady L, Balla T. Visualization and manipulation of plasma membrane-endoplasmic reticulum contact sites indicates the presence of additional molecular components within the STIM1-Orai1 Complex. J Biol Chem. 2007; 282:29678–29690. [PubMed: 17684017]

23. Huang GN, et al. STIM1 carboxyl-terminus activates native SOC, I_{crac} and TRPC1 channels. Nat Cell Biol. 2006; 8:1003–1010. [PubMed: 16906149]

24. Li Z, et al. Mapping the interacting domains of STIM1 and Orai1 in Ca^{2+} release-activated Ca^{2+} channel activation. J Biol Chem. 2007; 282:29448–29456. [PubMed: 17702753]

25. Miyawaki A, Griesbeck O, Heim R, Tsien RY. Dynamic and quantitative Ca^{2+} measurements using improved cameleons. Proc Natl Acad Sci U S A. 1999; 96:2135–2140. [PubMed: 10051607]

26. Miyawaki A, et al. Fluorescent indicators for Ca^{2+} based on green fluorescent proteins and calmodulin. Nature. 1997; 388:882–887. [PubMed: 9278050]

27. Griesbeck O, Baird GS, Campbell RE, Zacharias DA, Tsien RY. Reducing the environmental sensitivity of yellow fluorescent protein. Mechanism and applications. J Biol Chem. 2001; 276:29188–29194. [PubMed: 11387331]

28. Bautista DM, Hoth M, Lewis RS. Enhancement of calcium signalling dynamics and stability by delayed modulation of the plasma-membrane calcium-ATPase in human T cells. J Physiol. 2002; 541:877–894. [PubMed: 12068047]

29. Zweifach A, Lewis RS. Slow calcium-dependent inactivation of depletion-activated calcium current. Store-dependent and -independent mechanisms. J Biol Chem. 1995; 270:14445–14451. [PubMed: 7540169]

30. Prakriya M, Lewis RS. Potentiation and inhibition of Ca^{2+} release-activated Ca^{2+} channels by 2-aminoethyldiphenyl borate (2-APB) occurs independently of IP_3 receptors. J Physiol. 2001; 536:3–19. [PubMed: 11579153]

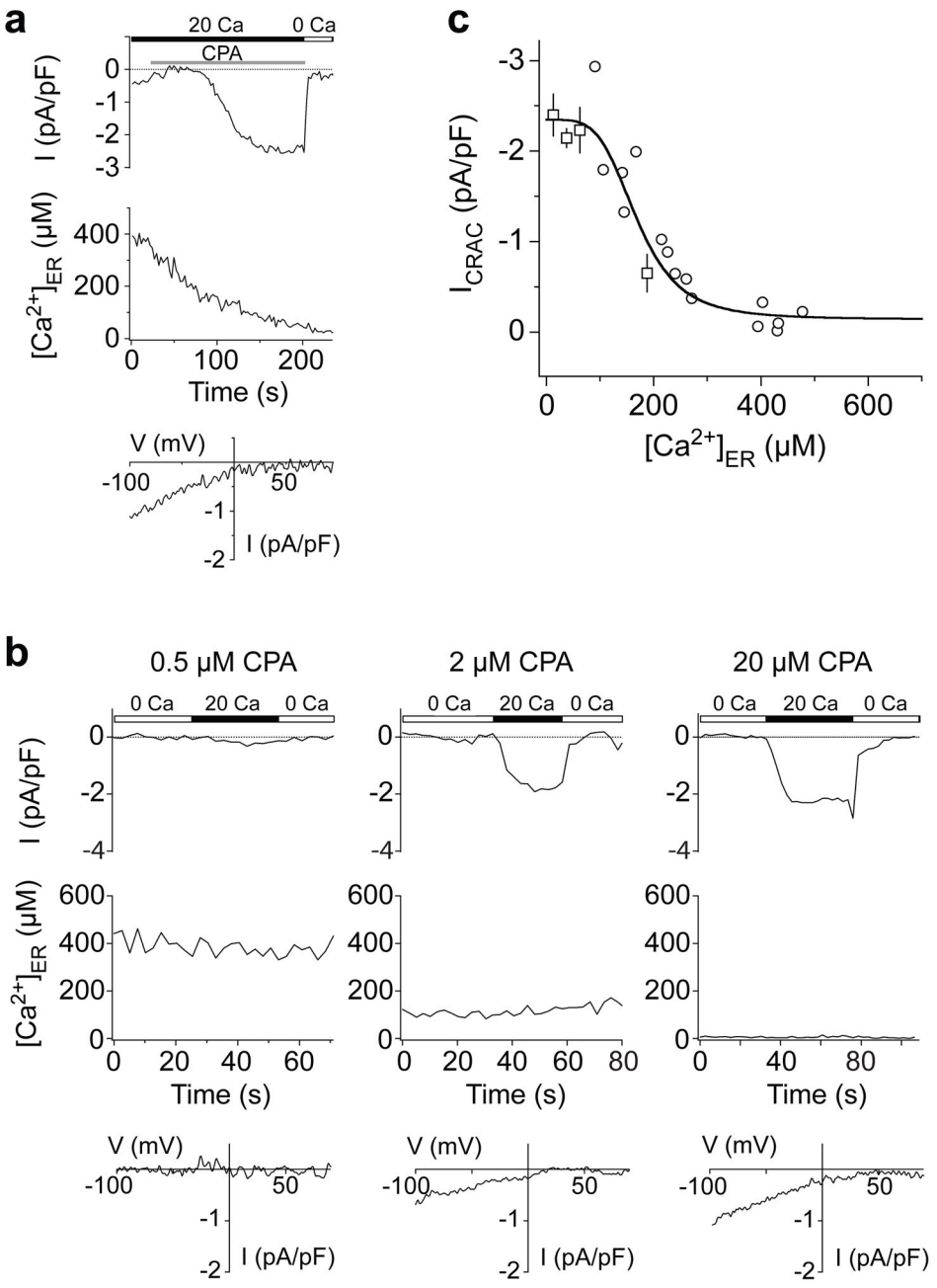

Figure 1. The $[Ca^{2+}]_{ER}$-response relation for the CRAC channel

Simultaneous measurements of $[Ca^{2+}]_{ER}$ and I_{CRAC} in individual Jurkat T cells. **a,** Non-stationary measurements of I_{CRAC} and $[Ca^{2+}]_{ER}$. Store depletion with 20 μM CPA induces an increase in I_{CRAC} (top) that follows a decrease in $[Ca^{2+}]_{ER}$ (middle) monitored with YC4.2er. The I-V relationship shows the inward rectification typical of I_{CRAC} (bottom). In this cell, a small inward current through outwardly-rectifying Cl^- channels is also present initially but disappears before I_{CRAC} is induced. **b,** Recordings of I_{CRAC} (top) and $[Ca^{2+}]_{ER}$ (middle) under steady-state conditions. Each cell was treated with the indicated CPA

concentration for 8–15 min prior to recording, and CPA was maintained throughout the experiment. I-V relations are typical for I_{CRAC} (bottom). **c,** Steady-state I_{CRAC} and $[Ca^{2+}]_{ER}$ are plotted for 40 cells after treatment with 0.5–20 μM CPA. A fit of the Hill equation with a $K_{1/2}$ of 169 μM and Hill coefficient of 4.2 is superimposed on the data. Squares: mean ± s.e.m. of 3–12 cells. Circles: single cells (see Supplementary Information).

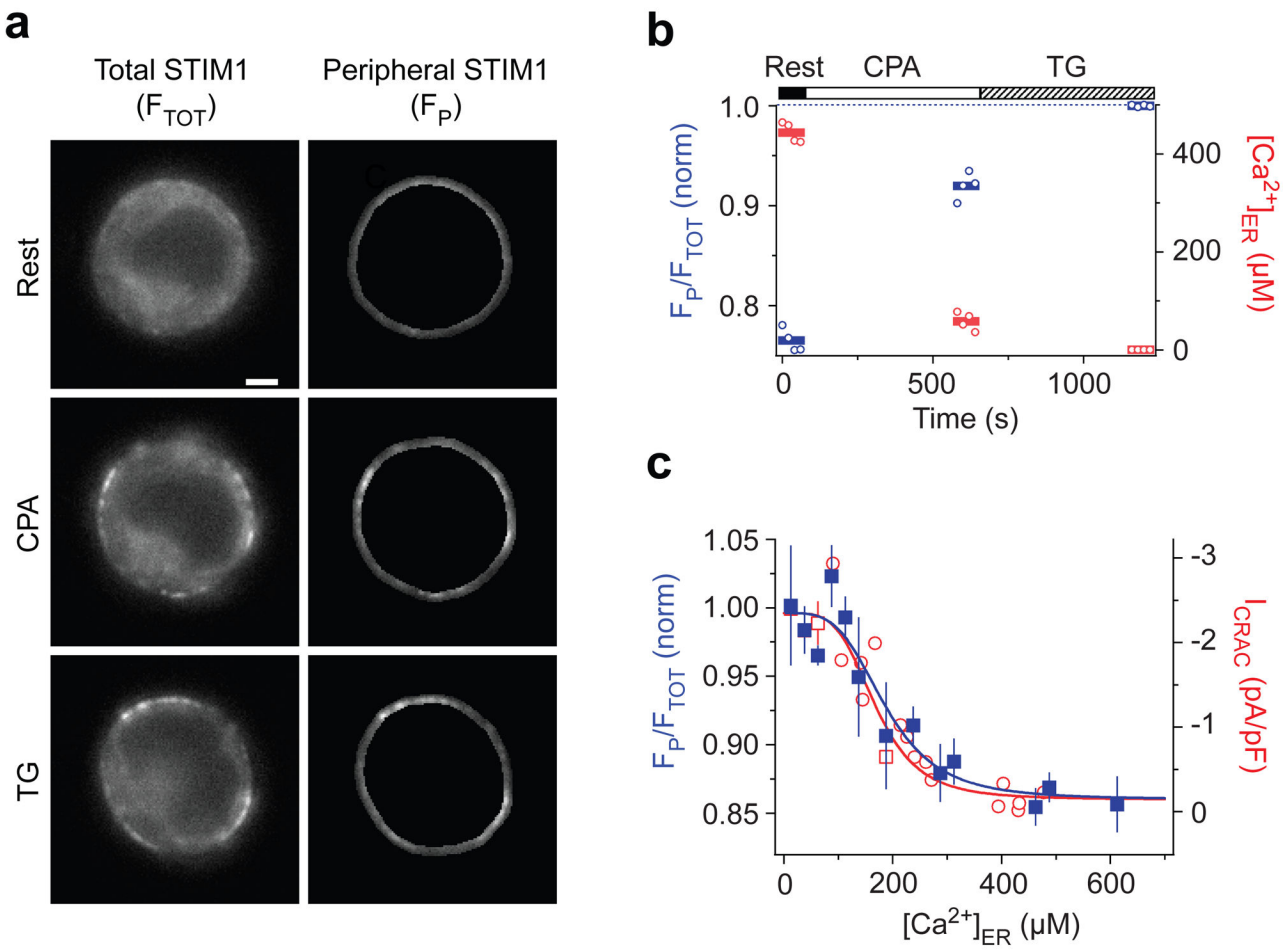

Figure 2. The $[Ca^{2+}]_{ER}$ dependence of STIM1 redistribution determines the $[Ca^{2+}]_{ER}$-response relation of the CRAC channel

a,Widefield epifluorescence images of a cell expressing Cherry-STIM1 at rest (top) and following store depletion with 3 μM CPA (middle) and TG (bottom). The redistribution of Cherry-STIM1 in single cells was monitored as the ratio of the mean Cherry fluorescence in the most peripheral 0.5 μm of the cell (F_P, right) to the mean fluorescence of the entire cell (F_{TOT}, left). Scale bar = 2μm. **b,** In the same cell, STIM1 redistribution represented by F_P/F_{TOT} normalized to the maximum ratio with TG (blue). F_P/F_{TOT} increases as $[Ca]_{ER}$ (red) declines. Individual data points (open symbols) and the mean response (bars) are shown. **c,** STIM1 redistribution ($F_P/F_{TOT,}$ blue) plotted against $[Ca^{2+}]_{ER}$ after treatment with 0–3 μM CPA (means ± s.e.m. of 3–4 cells; 41 cells total). A fit of the Hill equation (blue line) indicates a $K_{1/2}$ of 187 μM and Hill coefficient of 3.8. Steady-state I_{CRAC} data fitted with the Hill equation are re-plotted from Fig. 1 (red).

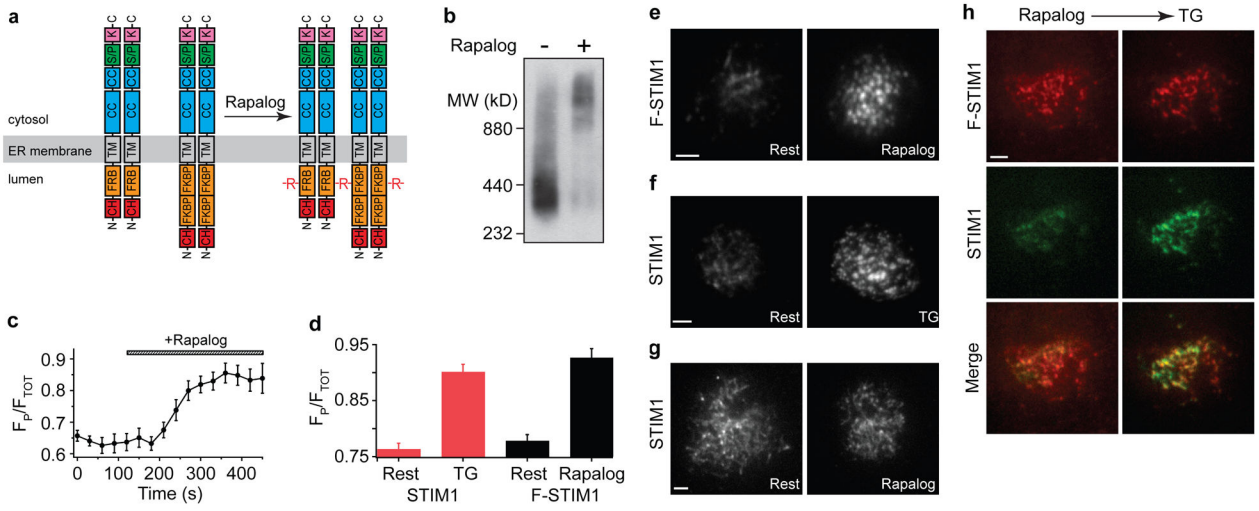

Figure 3. STIM1 oligomerization induces the accumulation of STIM1 at ER-plasma membrane junctions

a, The cartoon depicts the oligomerization of F-STIM1 induced by rapalog (R). At rest, FKBP-STIM1 and FRB-STIM1 are expected to form homo- and heterodimers; only intermolecular crosslinks between homodimers are shown here. Abbreviations: EF (EF hand), SAM (sterile-α motif), CC (coiled-coil), S/P (serine-proline-rich), K (lysine-rich), CH (mCherry). **b,** BN-PAGE and Western blot of transiently expressed F-STIM1 harvested from HEK293 cells. Untreated (left) and rapalog-treated (right) F-STIM1 was detected using a monoclonal anti-STIM1 antibody. **c,** Rapalog induces a time-dependent peripheral redistribution of F-STIM1 (n=10 cells). **d,** Peripheral redistribution of Cherry-STIM1 by TG (red bars; n=31 for each) and redistribution of F-STIM1 by rapalog (black bars; n=39, rest; n=42, rapalog). Values expressed as mean ± s.e.m. (**c, d**). **e–h**, TIRF images of Jurkat cells, scale bar = 2 μm. **e,** F-STIM1 before (left) and after (right) incubation with rapalog. **f,** Cherry-STIM1 before (left) and after (right) store depletion with TG. **g,** Cherry-STIM1 before (left) and after (right) incubation with rapalog. **h,** F-STIM1 (top row), GFP-STIM1 (middle row) and merged images (bottom row) from a single cell after rapalog treatment (left column) and subsequent store depletion with TG (right column). Cherry and GFP intensities are scaled to the maximal intensity of each fluorophore after TG treatment.

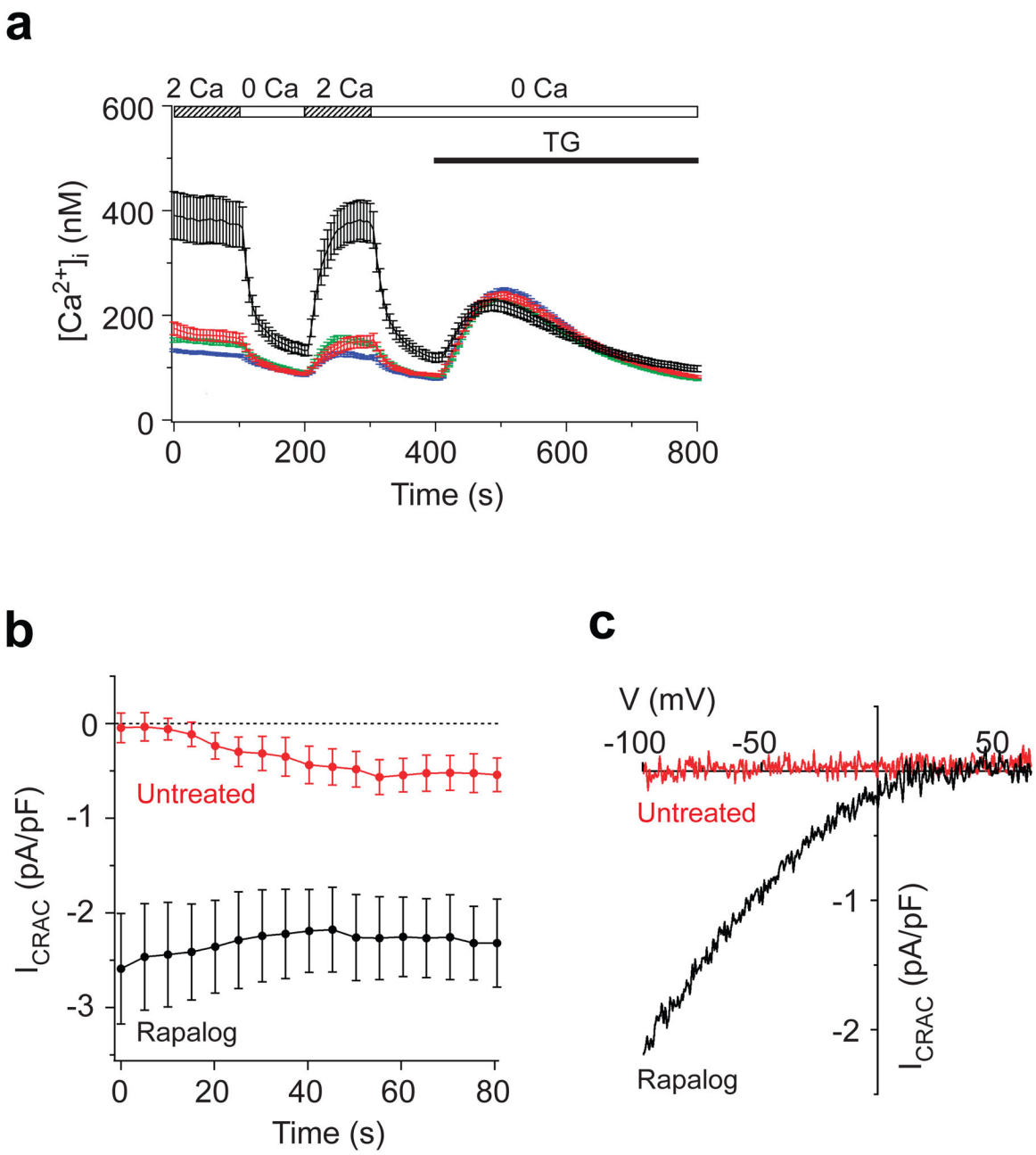

Figure 4. STIM1 oligomerization activates Ca^{2+} entry through CRAC channels

a, In rapalog-treated cells expressing F-STIM1 (black, n=45), resting $[Ca^{2+}]_i$ is elevated and sensitive to the removal of extracellular Ca^{2+}, indicating constitutive Ca^{2+} entry. In contrast, resting Ca^{2+} influx was largely absent in untreated F-STIM1-expressing cells (red, n=61) and in wt Jurkat cells with (green, n=617) or without (blue, n=517) rapalog. TG-induced Ca^{2+} release in rapalog-treated cells was similar to that of untreated cells. **b,** I_{CRAC} development during whole-cell recording from rapalog-treated (black, n=9) and untreated (red, n=9) cells expressing F-STIM1. I_{CRAC} was measured beginning within 5 s of break-in. **c,** I–V relations upon break-in, showing the inward rectification typical of I_{CRAC} in the

rapalog-treated cell (black) and the absence of current in the untreated cell (red). Values expressed as mean ± s.e.m. (**a,b**).